JOURNAL OF MATERIALS SCIENCE 21 (1986) 3445–3454

Analysis of second phase particles in a powder metallurgy HIP nickel-base superalloy

J. S. CROMPTON*, R. W. HERTZBERG
Department of Metallurgy and Materials Engineering, Whitaker Lab #5, Lehigh University, Bethlehem, Pennsylvania 18015, USA

The nature of the second phase particles associated with LC Astroloy prepared using powder metallurgy techniques has been examined. The individual particles have been identified using energy dispersive X-ray analysis and convergent beam electron diffraction. Four distinct types of particles have been observed: a cubic MC carbide in which M is either titanium or titanium plus molybdenum, a monoclinic phase ZrO_2, a trigonal α-Al_2O_3 and a tetragonal M_3B_2 phase in which M is molybdenum or molybdenum and chromium. The observations indicate that, although some MC carbides are associated with the ZrO_2 phase, the majority of the prior particle boundary precipitates are separate entities. Hot isostatic pressing or subsequent heat treatments above or below the γ' solvus were observed to have little effect on the incidence or distribution of the precipitation associated with the prior particle boundaries. In contrast, heat treatments above the γ'solvus resulted in the dissolution of the M_3B_2 phase and its preferential precipitation on the grain boundaries.

1. Introduction

The requirement for aerospace materials to operate under severe conditions of temperature and stress has led to a widespread interest in the optimization of microstructure to give the required mechanical properties. Generally, microstructures possessing a fine grained structure are required for good low cycle fatigue properties whereas coarse grained structures produce excellent crack propagation and creep resistance. Further changes in properties are often effected by heat treatments designed to control precipitation such that beneficial properties are developed. In conventionally produced materials, alloy development has concentrated on understanding the effects of various stages of the production schedule on the control of these microstructural variables.

More recently, interest has centred on the use of commercial powder metallurgy (PM) fabrication techniques of rapidly solidified material which virtually eliminate the potentially harmful segregation effects associated with conventionally cast materials. At the same time, the possibility of enhanced microstructural control is offered thus enabling improved component performance. Despite the obvious attractions of PM techniques some problems may be associated with its use in highly alloyed systems such as nickel-based superalloys. In addition to the problems associated with inherent porosity, detrimental mechanical properties may result from the undesirable nature of the precipitation on the original powder particle boundaries (PPBs) [1–3]. The precipitates may restrict grain growth of the material thus limiting the development of large grained materials; secondly, they cause a reduction in the amount of specific elements available for the precipitation of beneficial phases; and thirdly, the PPB precipitates themselves may be brittle and thus provide an easy fracture path. The nature of the precipitates and possible methods of controlling the precipitation behaviour are therefore of importance.

Analysis of the PPB precipitates is often restricted in view of the limitations of conventional EDX analysis to detect elements with atomic numbers less than 10. In many cases [2, 4, 5] the detection of elements such as titanium, niobium and molybdenum has led to the proposal that the particles are predominantly metal carbides of the form MC. Alternatively, surface analysis of the powder particles prior to compaction has revealed the presence of thin oxide layers [6, 7] leading to the suggestion that this preliminary surface oxidation aids the subsequent precipitation of MC. More specifically, Menzies *et al.* [8] have used their observations in PM IN100 to suggest that specific oxide particles act as nuclei for the formation of MC.

Some attempts to control the extent of PPB precipitation have been based upon making small compositional changes to the alloy. Reduction in the carbon content [1] or the inclusion of elements such as niobium, tantalum, hafnium [9, 10] or boron [11] have been made to halt the initial formation. In contrast, differing heat treatment procedures of the original alloys have been proposed to control PPB precipitation. Several investigators [12, 13] have suggested that hot isostatic pressing (HIP) at temperatures in excess of the γ' solvus reduces the extent of precipitation although the results of other workers [14, 15] do not support this viewpoint. Similarly, post HIP thermal treatments above the γ' solvus have also been

* *Present address*: Banbury Laboratories, Alcan International Ltd, Banbury, Oxon OX16 7SP, England.

0022–2461/86 $03.00 + .12

suggested as a means to control PPB precipitation [13, 16].

It has been the purpose of the present work to investigate the nature of the second phase particles present in a PM HIP nickel-based superalloy. To this end, detection methods based on the generation of X-ray spectra are limited either in terms of the elemental detection capabilities or, in the case of electron energy loss spectometry (EELS), in terms of the required specimen thickness [17]. A more efficient and direct guide to the precipitate's crystal structure and its related composition has been obtained by considering the nature of the diffraction from individual second phase particles. In addition, the influence of various heat treatments after powder compaction on the incidence and distribution of the PPB precipitates has also been investigated.

2. Material and experimental procedures

The material used in the present work was PM LC Astroloy, a nickel-based superalloy strengthened primarily by the presence of a coherent ordered γ' phase. The composition of the alloy is given in Table I. Powder of -140 mesh was produced by argon spray atomizing in an inert atmosphere; the material was then packed, sealed and treated with HIP in an inert atmosphere. All subsequent heat treatments were conducted in air. Heat treatments above and below the γ' precipitate solvus were investigated in the present alloy. Transmission electron microscopy (TEM) examination showed the γ' solvus to be in the range 1130 to 1140° C.

Specimens for optical metallography were polished and subsequently etched in either Kahling's reagent or a solution of 5% bromine in methanol. The majority of the analytical work was performed in thin foils produced by thinning with a commercial twin jet electropolishing unit using a solution of 10% perchloric acid, 45% acetic acid and 45% 2-butoxyethanol at room temperature and 50 V. To overcome background effects associated with general illumination of thin foils, some work was also performed on extraction replicas.

All work was conducted on a Philips EM400T operating at 120 kV and equipped with an EDAX 20° take-off angle X-ray detector and Tracor Northern 2000 multichannel analyser. Individual precipitate identification was made using convergent beam diffraction (CBD) analysis whilst energy dispersive X-ray spectra (EDX) were generated to specifically identify the heavier elements involved in the precipitate. EDX spectra were recorded in the 0 to 20 keV range to allow higher energy K peaks to be observed. A probe size less than the particle size was used and analysis conducted for times between 60 and 100 sec; the total counts recorded depended on precipitate size, thickness and tilt angle.

Convergent beam diffraction patterns (CBDPs) were generated by either effecting adjustments to the condenser and objective lenses to produce a fine crossover at the specimen plane or in scanning transmission electron microscopy (STEM) by merely stopping the electron beam scanning the specimen. Analysis of CBDPs may be conducted in several ways. The approach favoured by Steeds and co-workers [18–20] related the symmetry elements present in the diffraction patterns to the crystal's point and space group. Alternatively, Raghavan *et al.* [21] have utilized the information of interplanar spacings and angles to identify phases. More recently, comparison of unknown patterns with those generated by known phases has become possible [22]. All of these approaches were used here depending on the nature of the information available in the CBDP.

3. Results and discussion

The research undertaken here was designed to identify the nature of the second phase particles present in the PM LC Astroloy and to study the influence of simple heat treatments. The potentially detrimental nature of precipitation on PPBs can be appreciated in Fig. 1. Although small grain sizes may be easily developed, in this case HIP at 1107° C for 2 h followed by annealing at 1123° C for 2 h resulted in a grain size of 5 μm, PPB precipitation superimposes a larger scale structure on the alloy. The circular areas (e.g. A in Fig. 1) represent cross-sections of the original powder particles whose position is revealed due to preferential etching of the PPB precipitates. The size of the cross-section varies considerably but the maximum size that was observed compared favourably with that expected from the mesh size used for alloy preparation.

Examination of the material in thin foils (Fig. 2) shows the nature of the microstructure more clearly. In addition to the cuboidal γ' precipitates, precipitation associated with the PPBs may be seen at the junction of three powder particles. In general, the PPB precipitates varied in size from ~ 0.3 to 0.02 μm with spacings of the same order. Initial attention will be focused on the identification of these second phase particles, with results then presented to reveal the influence of various heat treatments on the nature and distribution of these precipitates.

TABLE I Alloy composition (wt%)

Co	Cr	Mo	Al	Ti	Fe	Zr	B	C	Si	Mn	Cu	W
16.98	14.8	5.07	3.99	3.58	0.21	0.047	0.026	0.024	0.02	0.01	0.01	0.01

P	N	S	Ni	O*
0.003	0.002	0.001	balance	< 170 p.p.m.

*Oxygen by analysis of air exposed powder.

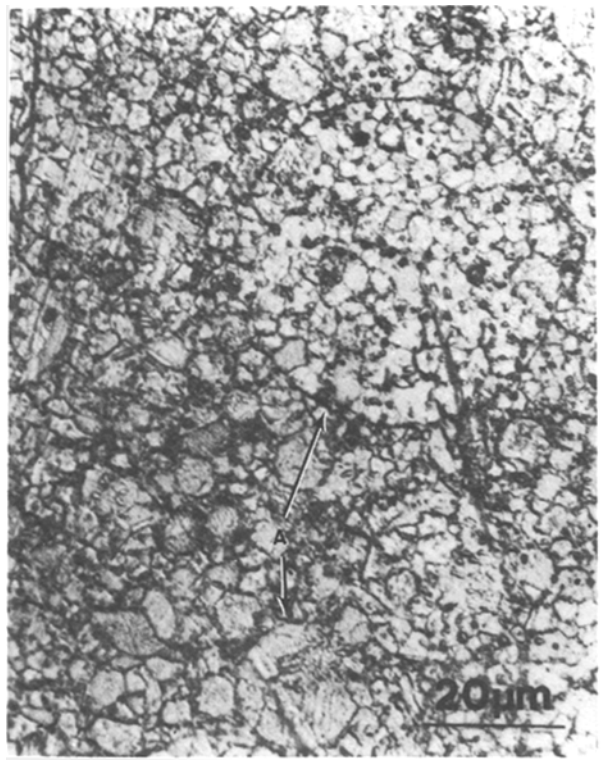

Figure 1 Optical micrograph of material HIP at 1107° C for 2 h, annealed at 1123° C for 2 h and aged at 650° C for 24 h. PPBs shown at A.

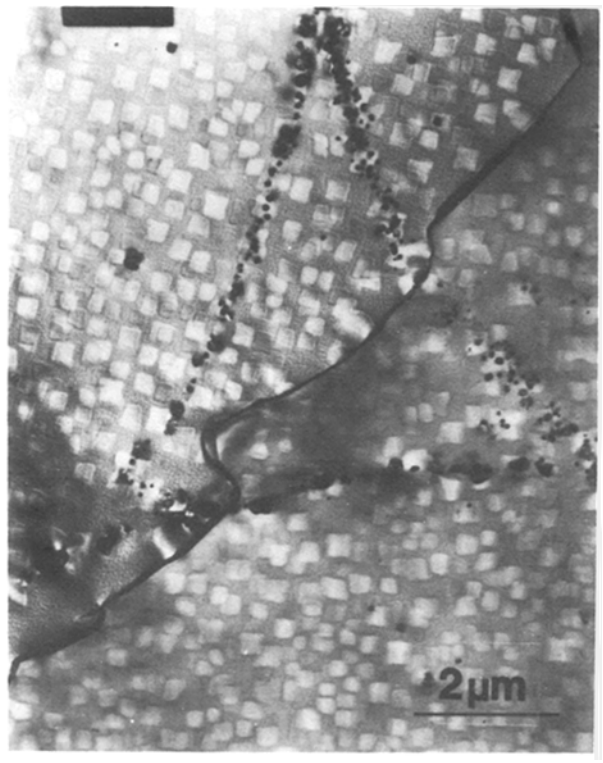

Figure 2 TEM micrograph showing the precipitation on the PPBs at the junction of three powder particles. Specimen HIP 1107° C for 2 h.

3.1. Phase identification

Analysis of the precipitates revealed that although the constituent elements varied considerably they could be conveniently grouped into four major types. In the first type, EDX analysis revealed the presence of considerable amounts of titanium (Fig. 3); the other peaks present are due to the spurious generation of X-rays from matrix material adjacent to the precipitate. In general, these precipitates were disc shaped with a size of approximately 0.1 μm and were readily electron transparent. More specific identification of the phase may be obtained by a consideration of the low index zone axis CBDPs generated from the individual precipitates (Fig. 4). The symmetries of the zero order Laue zone (ZOLZ) and higher order Laue zones (HOLZs) may be used to determine the possible diffraction groups of the crystalline phase which may in turn be related to the crystal's point and space group [18–20, 23] thus permitting phase identification. A consideration of the symmetries exhibited in this case enabled possible ambiguities to be eliminated and the crystal point group to be identified as m3m. Analysis of the diffraction information for the ZOLZ and first order Laue zone (FOLZ) further enables the indexing of individual diffraction maxima for the zone axes in terms of the cubic phase MC; for this case M is titanium, with the MC carbide having a lattice parameter approximately 0.43 nm.

As a further check, the reciprocal lattice layer spacing in the direction of the electron beam, H, was compared with the corresponding real space value. The magnitude of H can be evaluated from the radius of the FOLZ ring, G, as described by Steeds [18]

$$H = \frac{G^2\lambda}{2} \quad (1)$$

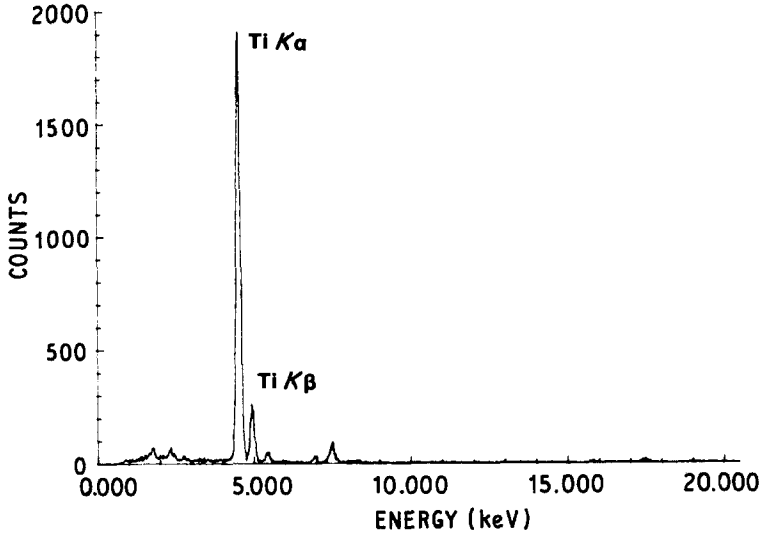

Figure 3 EDX analysis of PPB precipitate in material HIP at 1107° C for 2 h, solution treated at 1149° C and aged at 650° C for 24 h.

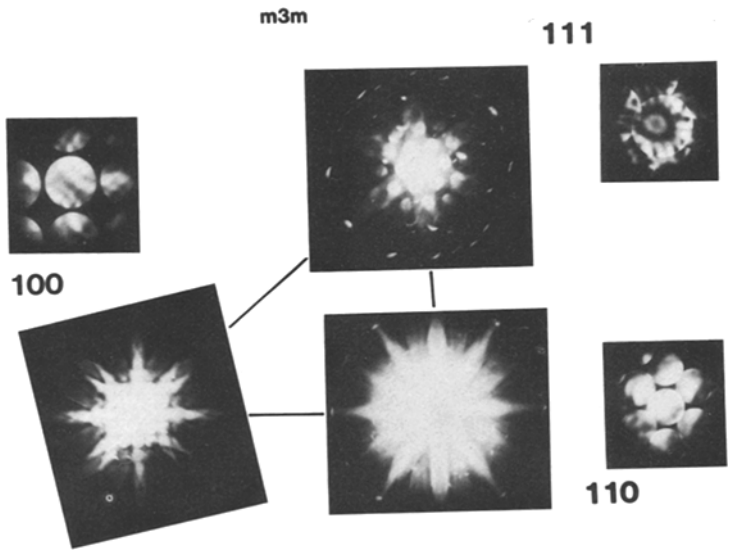

Figure 4 CBDP zone axis map for MC carbide with the point group m3m generated from precipitates with EDX spectrum of Fig. 3.

where G (nm^{-1}) = $R/\lambda L$, R is the radius of the FOLZ ring in cm, λL is the camera constant in cm nm and λ is the wavelength of the electrons. The value of H^{-1} may then be related to the real lattice through simple geometric relationships [21]. In the present case, the experimentally determined value of 0.435 nm for the ⟨0 0 1⟩ zone axis compares favourably with the expected value of 0.4328 nm expected for TiC [24]. In a similar manner, second phase particles containing titanium and molybdenum (Fig. 5) were observed and identified as belonging to the MC class where M is then titanium and molybdenum.

Occasional EDX analysis of particles generated spectra which indicated the presence of both titanium and zirconium (Fig. 6). Detailed examination of these particles revealed them to be essentially two precipitates (Fig. 7). EDX analysis of one part gave spectra similar to Fig. 3 in which titanium was the predominant element whereas the other part generated EDX spectra containing zirconium (Fig. 8). In addition, numerous individual particles containing zirconium were found and convergent beam patterns similar to Fig. 9 generated. Comparison of the lattice parameter information and reciprocal lattice layer spacing from these diffraction patterns with lattice information for standard phases available in powder diffraction file information enables the patterns to be consistently and unambiguously indexed and the phase identified as monoclinic zirconia, ZrO_2.

In the situation where two precipitates were associated (Fig. 7) the titanium rich phase was identified as MC, whereas the zirconium rich phase was ZrO_2. The co-existence of these phases has been previously suggested by Menzies *et al.* [8] using EELS analysis in IN100. They have suggested that the ZrO_2 particles act as nuclei for the subsequent formation of MC which then envelopes the ZrO_2 nucleus. Although the co-existence of both the MC and ZrO_2 phases was noted in the present work, by far the greater number of ZrO_2 and MC particles were found in isolation (Fig. 10). In Fig. 10 it can be seen that in one case ZrO_2 and MC are combined but in the majority of the cases the phases are separate. It is unlikely that this observation is confused by preferential particle loss during specimen preparation since EDX analysis in regions adjacent to isolated zirconia particles, using fine probe sizes, failed to show local increases in either titanium or molybdenum levels. Similarly, analysis across and close to isolated MC particles failed to show increased levels of zirconium. This suggests that, even if MC nucleates on zirconia particles, the existence of ZrO_2 is not a sufficient criterion for the formation of MC.

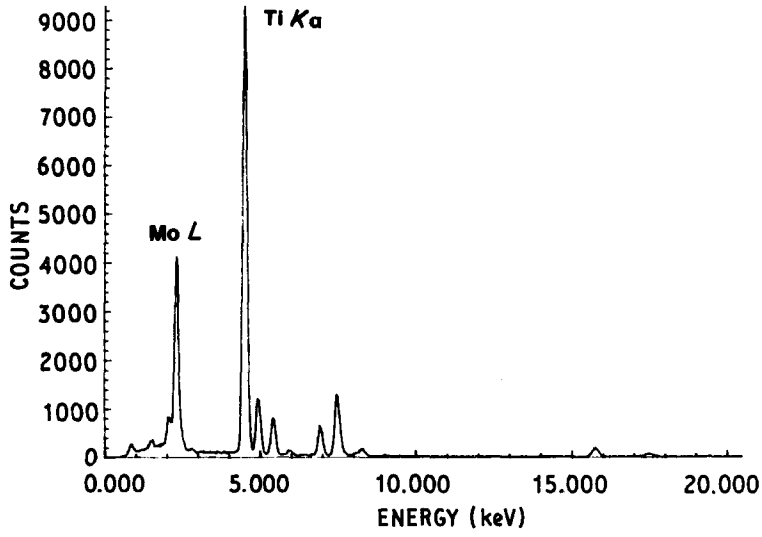

Figure 5 EDX analysis of MC carbide showing presence of titanium and molybdenum.

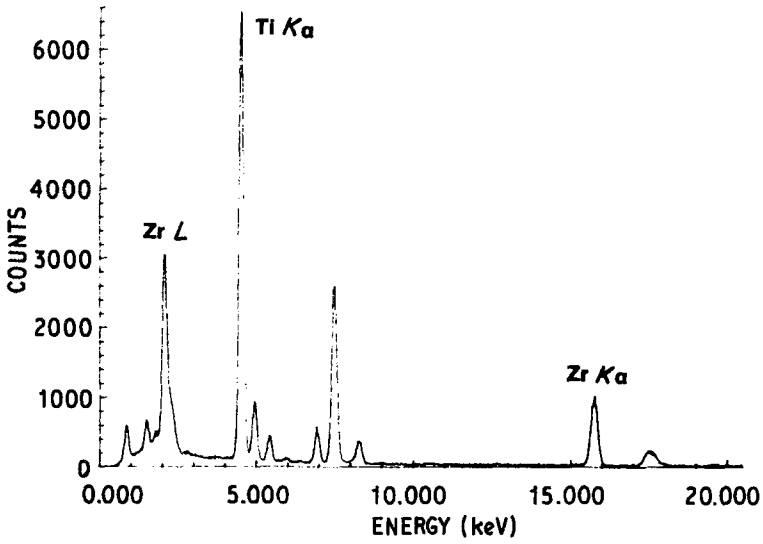

Figure 6 EDX analysis of particles showing presence of titanium and zirconium.

The EELS analysis of Menzies *et al.* [8] also suggested the existence of TiO_2 and Al_2O_3 phases both of which were similarly proposed to act as nuclei for MC formation. In the present material no observations of TiO_2 were made but numerous particles with EDX spectra displaying aluminium K_α and K_β peaks were found (Fig. 11); CBDPs from this phase (Fig. 12) confirmed this phase as trigonal α-Al_2O_3. In none of the cases examined was an association between α-Al_2O_3 and MC carbides observed.

In addition to the small precipitates obviously associated with the PPBs much larger precipitates were observed (Fig. 13). These were generally of a blocky morphology with sizes ranging from 0.5 to 0.1 μm, and although some were located close to original powder surfaces many were apparent within the areas ascribed to the body of a powder particle. EDX analysis of these phases showed them to be composed primarily of molybdenum or molybdenum and chromium (Fig. 14). Exact analysis of this phase was obtained using CBDPs typical patterns can be seen in Fig. 15. In Fig. 15a, 2 mm symmetry of both ZOLZ and HOLZ is exhibited whereas Fig. 15b displays 4 mm symmetry. In addition, the ZOLZ of Fig. 15b shows the existence of dark bars in the horizontal and vertical spots which represent lines of dynamic absences [15, 25] and indicate the presence of both screw axes and glide planes. These features, together with other patterns indicate a point group of 4/m m m and a space group of P4/m b m thus establishing the precipitate as a tetragonal phase M_3B_2 in which M is molybdenum or Mo + Cr.

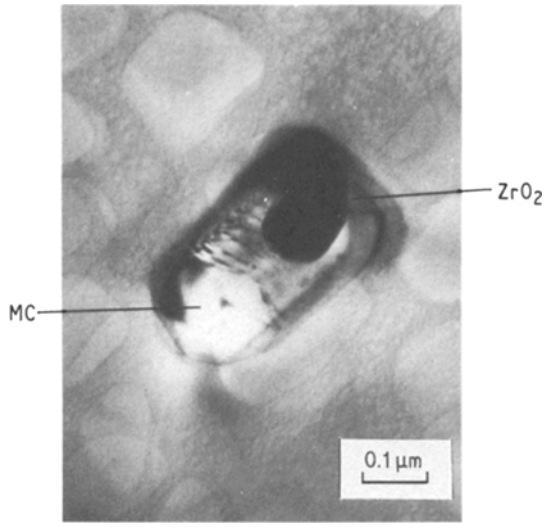

Figure 7 TEM micrograph of precipitate with spectrum of Fig. 6 showing two distinct phases identified as MC and zirconia (ZrO_2).

The formation of this phase in itself may be considered detrimental. For the most part boron is added to superalloys to enhance high temperature ductility, which is generally thought to be due to the preferential segregation of boron in the alloys. Clearly in this alloy boron is found in large precipitates such that the benefits of the preferential segregation are not obtained so that high temperature properties may no longer be optimized. Additionally, the presence of these large precipitates may by itself be detrimental by permitting crack nucleation or high temperature cavitation.

A substantial body of research [6, 7] has indicated that, despite the use of inert atmospheres for atomization, oxidation may give rise to a thin oxide film ($\cong$ 20 nm) on the powder surface. It has been further suggested [6] that this film may enhance subsequent precipitation and specifically MC precipitation, either prior to or during compaction leading to the decoration of the PPBs. Although the present research does not show whether MC precipitates during atomization or compaction it does indicate that, although some MC particles may be linked to zirconia precipitates, by far the larger proportion were separate particles. Further, the majority of the oxides whether ZrO_2 or α-Al_2O_3 were also discrete entities.

The conditions required for the formation of ZrO_2 and α-Al_2O_3 may be examined by consideration of the partial pressure of oxygen required for their formation. This value may be obtained by use of the thermodynamic relationship.

$$\Delta G_{ox} = -RT \ln K_p \qquad (2)$$

in which ΔG is the free energy change for oxide formation at a temperature T, R is the gas constant and K_p is the equilibrium constant $= \alpha_{ox}/\alpha_M p_{O_2}$ for which α_{ox} is the oxide activity assumed to be unity, α_M is the metal activity assumed equal to its molar fraction and

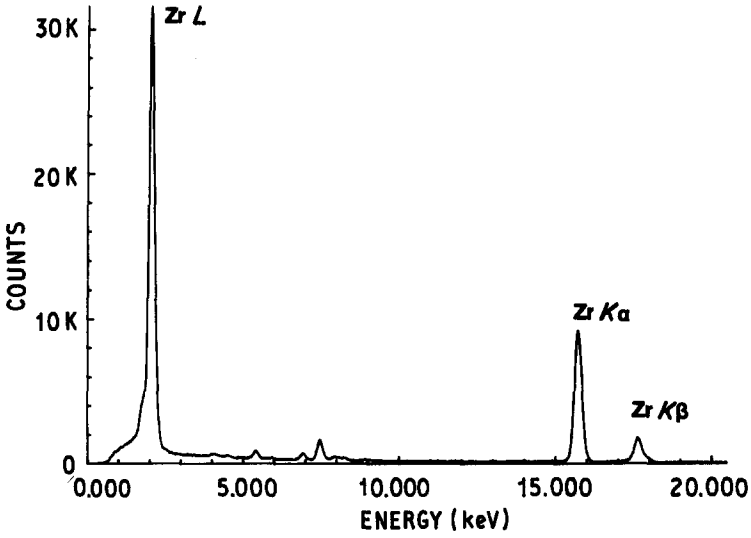

Figure 8 EDX analysis of zirconia phase.

p_{O_2} is the partial pressure of oxygen. Using temperature corrected free energy values [26] for a typical atomization temperature close to the melting point of nickel (1728 K) and a typical HIP temperature of 1280 K p_{O_2} values may be obtained. For α-Al_2O_3 values of 3.5×10^{-30} Pa at 1280 K and 2.8×10^{-18} Pa at 1728 K are indicated whereas ZrO_2 yields values of 3.9×10^{-30} and 6.6×10^{-19} Pa, respectively.

Thus it can be seen that oxide formation is always likely to take place during powder atomization processing and it is unlikely that sufficient atmospheric control can be exercised to eradicate oxide formation. Should elimination of ZrO_2 and α-Al_2O_3 be possible it is improbable that this will eradicate PPB precipitation. Although MC has been observed in conjunction with ZrO_2, the majority of the MC carbides were observed as discrete particles. Hence it becomes necessary to consider separate means by which MC precipitation and ZrO_2 and α-Al_2O_3 formation may be restricted. The latter operation remains difficult in view of the restriction imposed by the required p_{O_2} levels and further calculations which indicate that preferential oxidation of other elements may ensue. In contrast, control of MC precipitation may be effected by enhanced compositional control such as drastic reduction in carbon level. However, even if MC precipitation were eliminated this would merely result in a reduction in the number of particles on the PPB and not completely eliminate them. Alternative methods of controlling PPB precipitation have centred on the use of heat treatment procedures; an investigation into the effects of simple heat treatments forms the second part of this work.

3.2. Influence of heat treatment procedure

Various heat treatment schedules above and below the solvus temperature of the γ' precipitate have been

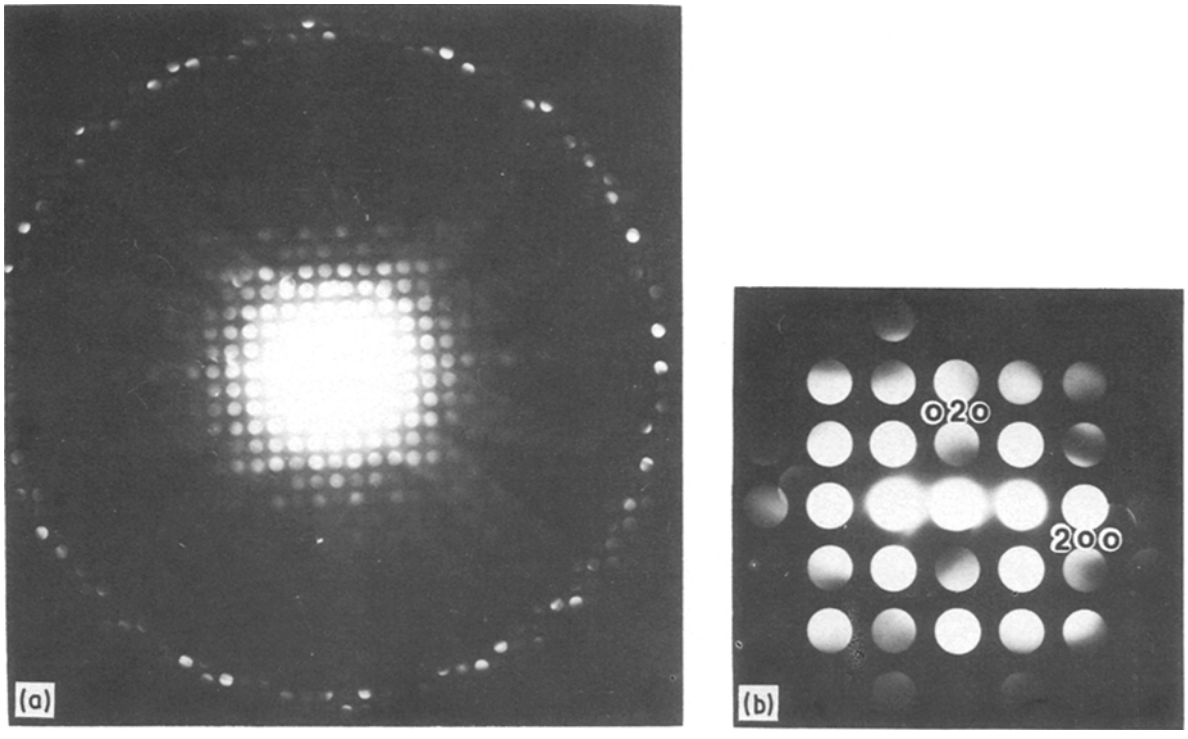

Figure 9 CBDPs from monoclinic zirconia precipitate, beam direction [0 0 1].

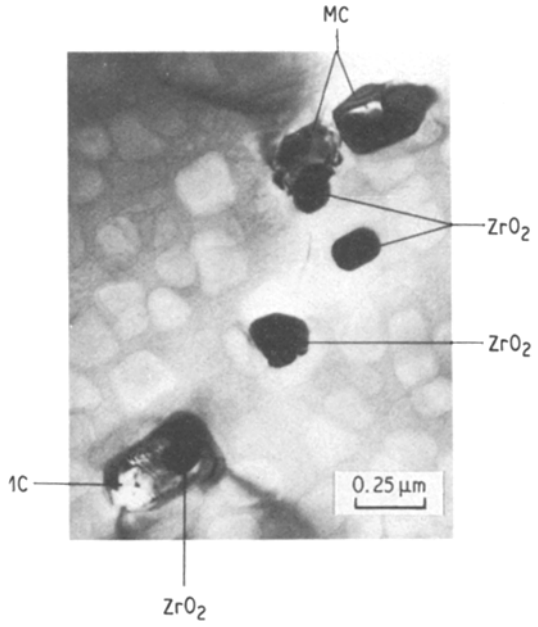

Figure 10 TEM micrograph showing MC and ZrO_2 precipitation on the PPBs. In some instances the two phases appear connected, in most cases, however, the phases are separate.

attempted. For the present alloy the solvus temperature was determined to be in the range 1130 to 1140° C. In general, heat treatments were found to have little noticeable effect on the PPB particles; HIP above or below the γ' solvus resulted in the presence of the numerous PPB particles identified earlier. Similarly heat treatments after compaction failed to alter the nature of the PPB particles or to significantly reduce either their number or spacing.

For the major part, the changes in the distribution of the PPB particles were not associated with changes in the precipitates themselves but rather due to microstructural changes resulting from the heat treatment procedures used. HIP and/or subsequent heat treatment above the γ' solvus resulted in a considerable amount of grain growth. As a result, the number of grains containing PPB particles decreases and, as the grain size increases, an increase in the number of PPB particles lying on the grain boundary was observed. Situations where grain growth was sufficiently impeded by PPB particles to halt subsequent grain boundary motion were rare. It is thought that this may merely represent the fact that the driving force for grain growth is continually decreasing so that in most cases the grain boundaries do not approach surrounding PPB particles. Whilst the observations on the incidence of PPB particles following heat treatments are counter to those reported by Prakash *et al.* [13], they are not surprising since the PPB precipitates (MC, ZrO_2 and α-Al_2O_3) are stable over the temperature range investigated here, 1107 to 1246° C. Indeed, zirconia is stable up to 2680° C although it exhibits changes in crystal structure at various temperatures up to this level. Therefore, it is not surprising that heat treatments after atomization lead to no observable change in the incidence of PPB precipitates.

In contrast to the small PPB particles, the other major phase observed in the present work (M_3B_2) revealed changes in its distribution as a result of heat treatments. In specimens HIP and/or heat treated below the γ' solvus, the boride particles remained large and blocky (see Fig. 13); material heat treated above the γ' solvus failed to show this distribution. In these materials the boride phase was observed to lie predominantly along the grain boundaries. The features of these materials can be seen in Fig. 16. Despite the elevated temperature treatment imposed on this specimen, the features of PPB precipitation are evident. Individually identified precipitates are shown and it is clear that the phases associated primarily with the PPBs, i.e. MC, ZrO_2 and α-Al_2O_3, remain in evidence. It is also clear that the boride phases are predominantly associated with the grain boundaries.

It has been reported [11] that the solution treatment temperature of the boride phases is approximately 1100° C and that ageing at 850° C results in reprecipitation. Material HIP and/or heat treated below 1121° C showed a block M_3B_2 morphology located both intergranularly and intragranularly. However, material HIP and/or subsequently heat treated above 1149° C gave M_3B_2 located primarily on grain boundaries, thus suggesting that in the present alloy, the solution treatment temperature of the boride phases is somewhere in the range 1121 to 1149° C. This further

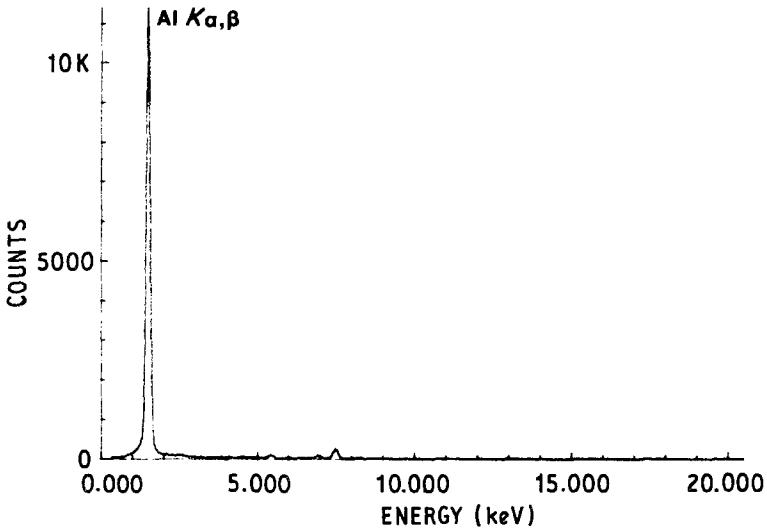

Figure 11 EDX analysis of one of PPB precipitates showing aluminium $K\alpha$ and $K\beta$ peaks.

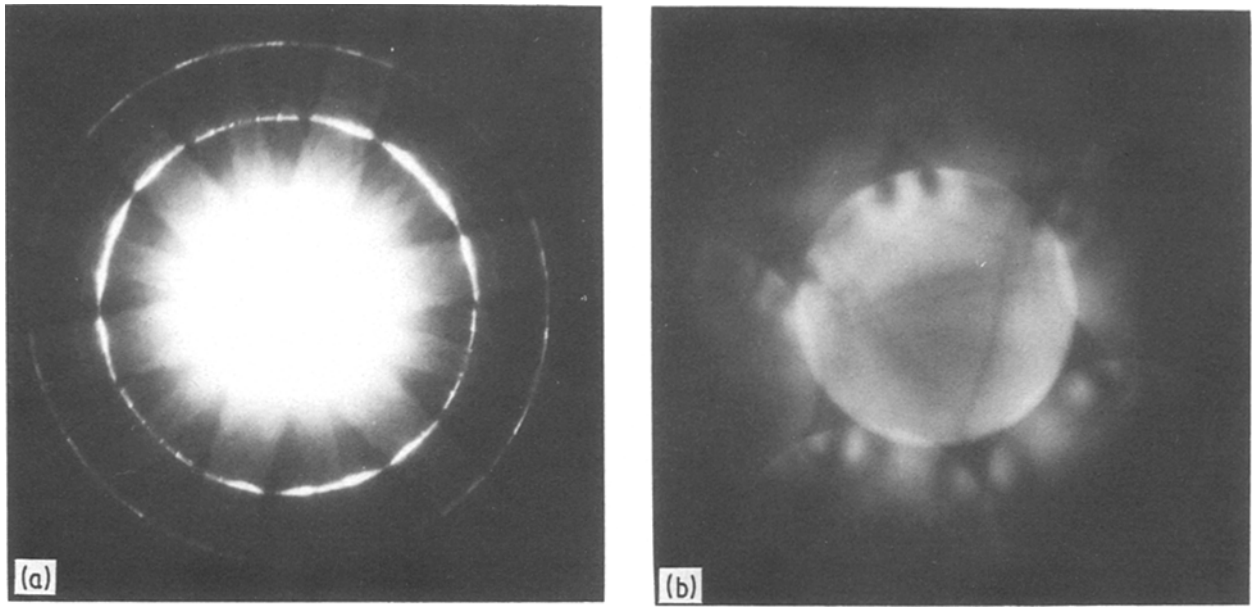

Figure 12 CBDPs from precipitate having EDX spectrum of Fig. 11 showing HOLZ contrast in the zero order disc with 3 m symmetry. Full analysis indicates the patterns are from trigonal α-Al_2O_3 with a beam direction [0 0 0 1].

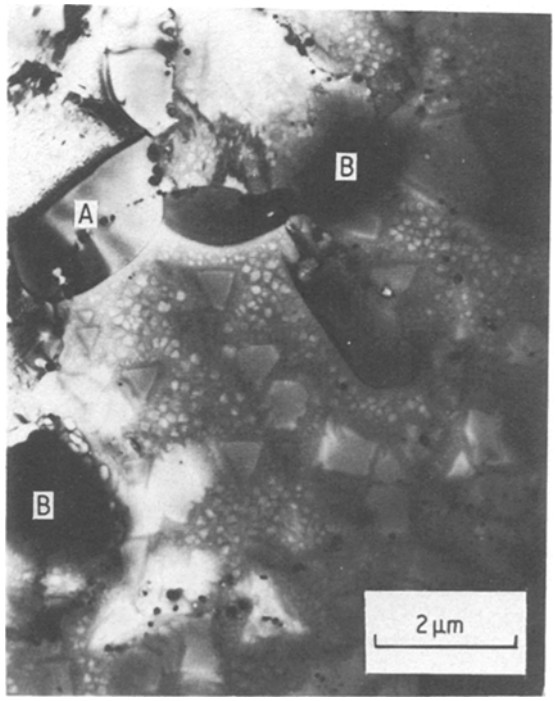

Figure 13 TEM micrograph showing PPB precipitation (A) together with larger blocky precipitates (B).

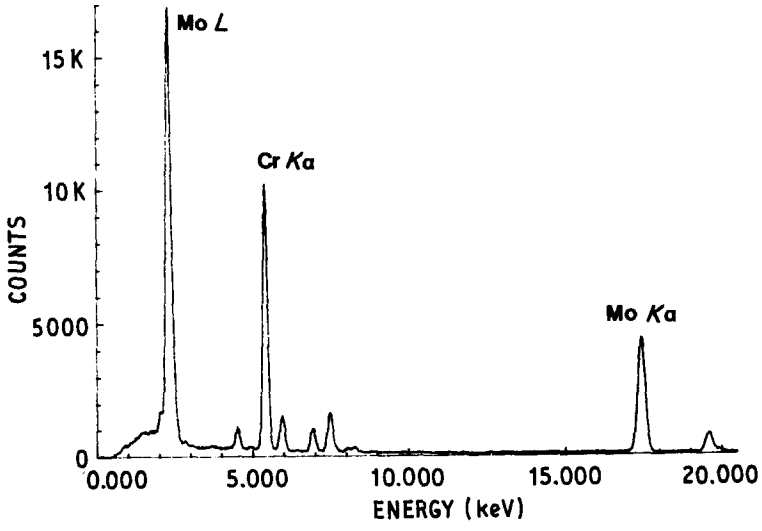

Figure 14 EDX analysis of blocky precipitates of Fig. 13 showing presence of both molybdenum and chromium.

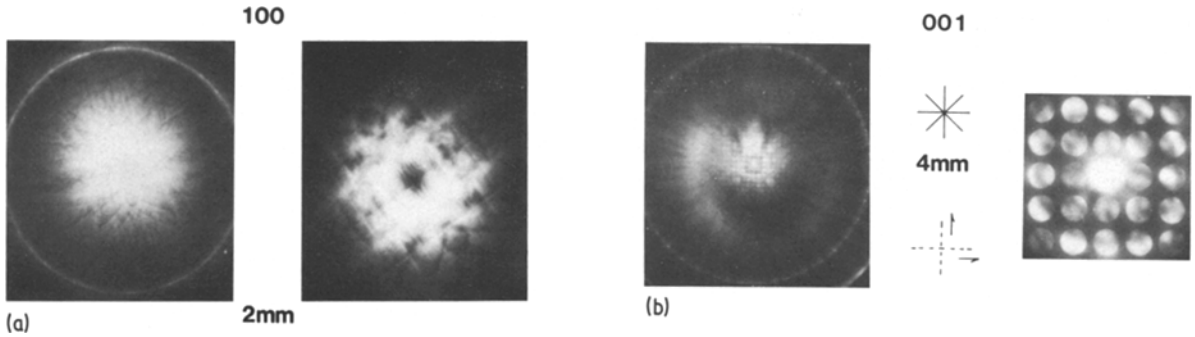

Figure 15 CBDPs from particles with EDX analysis of Fig. 14 showing (a) 2 mm symmetry and (b) 4 mm symmetry and dynamic absences in $\pm(1\,0\,0)$ and $\pm(0\,1\,0)$ reflections due to both screw axes and glide phases. These patterns result from the primitive tetragonal M_3B_2 phase with a point group of 4/m m m and space group of P4/m b m in which M is molybdenum and or molybdenum and chromium.

indicates that the M_3B_2 phase may be present in the initial rapidly solidified powder in material subjected to the lower temperature since it is located randomly throughout the material whereas material heat treated above 1149° C results in dissolution of M_3B_2 which reprecipitated on grain boundaries on cooling thus giving the characteristic distribution observed.

4. Conclusions

The work described here has identified numerous second phase particles associated with a powder formed superalloy and has studied their nature as a function of the heat treatments employed. The major conclusions from this work are:

1. The precipitates associated with the powder particle boundaries are generally in the size range 0.3 to 0.02 μm and have been found to be composed of three basic types: (i) MC – a cubic carbide in which M is Ti or Ti + Mo; (ii) ZrO_2 – a monoclinic phase; (iii) α-Al_2O_3 – a trigonal phase.

2. Larger precipitates with sizes up to 0.5 μm were found and identified as M_3B_2 in which M has been shown to be Mo or Mo + Cr.

3. Although several MC and ZrO_2 precipitates were found in conjunction the majority were separate entities, indicating that MC precipitation takes place primarily in the absence of a ZrO_2 nucleus.

4. Heat treatments above or below the γ' solvus were observed to have little effect on the incidence of the PPB precipitates.

5. Heat treatments above the γ' solvus resulted in dissolution and subsequent reprecipitation of the M_3B_2 phase on the grain boundaries.

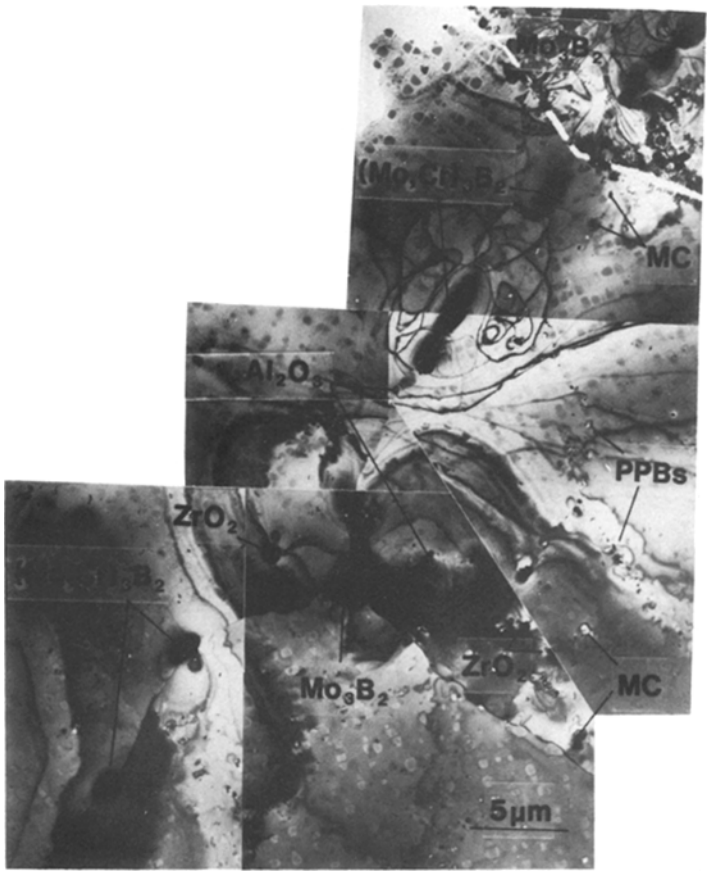

Figure 16 TEM micrograph of material HIP at 1246° C for 2 h, solution treated at 1150° C for 2 h and aged at 1100° C for 4 h. Despite the heat treatments above the γ' solvus PPB precipitation is still in evidence with individual precipitates of MC, ZrO_2 and α-Al_2O_3 shown. Extensive precipitation of M_3B_2 on the grain boundaries may be seen.

Acknowledgements

The authors would like to thank the US Air Force for financial support under grant number AFOSR-83-0029. In addition, the technical co-operation of Carpenter Technology, Reading, Pennsylvania and IMT Corporation, Andover, Massachusetts is greatly appreciated.

References

1. N. M. ALLEN, R. L. ATHEY and J. B. MOORE, in "Progress in Powder Metallurgy", Vol. 31, edited by G. D. Smith (Metal Powder Industries Federation, Princeton, New Jersey, 1975) p. 243.
2. J. M. LARSON, in "Modern Developments in Powder Metallurgy", Vol. 8, edited by H. H. Hausner and W. E. Smith (Metal Powder Industries Federation, Princeton, New Jersey, 1974) p. 537.
3. J. BRESSERS, M. ROTH, E. FENSKE and P. TAMBUYSER, in "Proceedings of the International Symposium on High Temperature Materials for Gas Turbines" edited by P. Coutsouradis, Liège, Belgium (Elsevier, 1982) p. 597.
4. N. G. INGESTEN, R. WARREN and L. WINBERG, in "Proceedings of the International Symposium on High Temperature Materials for Gas Turbines" edited by P. Coutsouradis, Liège, Belgium (Elsevier, 1982) p. 1013.
5. C. AUBIN, J. M. DAVIDSON and J. P. TROTTIER, in "Proceedings of the 4th Symposium on Superalloys" edited by J. K. Tien, S. T. Wlodek, H. Morrow, M. Gell and G. E. Maurer (American Society for Metals, Seven Springs, Pennsylvania, 1980) p. 345.
6. R. E. WATERS, J. A. CHARLES and C. LEA, *Met. Technol.* (1981) 194.
7. R. WARREN, N. G. INGESTEN, L. WINBERG and T. RÖNNHULT, *Powder Met.* **27** (1984) 141.
8. R. G. MENZIES, R. H. BRICKNELL and A. J. CRAVEN, *Phil. Mag. A* **41** (1980) 493.
9. G. J. LEWIS, D. M. PARKIN and F. A. THOMPSON, in "Proceedings on the Conference on Forging and Properties of Aerospace Materials" (Metals Society, London, 1978) p. 399.
10. R. D. ENG and D. J. EVANS, in "Proceedings of the 4th Symposium on Superalloys" edited by J. K. Tien, S. T. Wlodek, H. Morrow, M. Gell and G. E. Maurer (American Society for Metals, Seven Springs, Pennsylvania, 1980) p. 491.
11. C. A. HAMMERSLEY, *Metallurgia* **45** (1978) 105.
12. M. J. BLACKBURN and R. A. SPRAGUE, *Met. Technol.* **4** (1977) 388.
13. T. L. PRAKASH, Y. N. CHARI, E. S. BHAGIRADHA RAO and R. THOMBURAJ, *Metall. Trans.* **14A** (1983) 733.
14. M. T. PODOB, in "Modern Developments on Powder Metallurgy", vol. 11, (Metal Powder Industries Federation, Princeton, New Jersey, 1977) p. 25.
15. P. E. PRICE, R. WIDMER and J. C. RUNKLE, in "Modern Developments in Powder Metallurgy", vol. 11 (Metal Powder Industries Federation, Princeton, New Jersey, 1977) p. 45.
16. R. THOMBURAJ, W. WALLACE, Y. N. CHAM and T. L. PRAKASH, *Powder Metall.* **27** (1984) 169.
17. D. B. WILLIAMS, in "Practical Analytical Electron Microscopy in Materials Science (Philips Electronic Instruments, Manwah, New Jersey, 1984) p. 91.
18. J. W. STEEDS, in "Introduction to AEM", edited by J. J. Hren, J. I. Goldstein and D. C. Joy (Plenum Press, New York, 1979) Ch. 15.
19. J. W. STEEDS, G. M. RACKHAM and M. D. SHANNON, Institute of Physics Conference Series No. 41 (Institute of Physics, London, 1979) p. 135.
20. L. P. STORER, *J. Mater. Sci.* **16** (1981) 1356.
21. M. RAGHAVAN, J. Y. KOO and R. PETKOVIC-LUTON, *J. Met.* **35** (1983) 44.
22. The Bristol Group, Convergent Beam Electron Diffraction of Alloy Phases, compiled by J. Mansfield (Adam Hilger, Bristol, 1985).
23. B. F. BUXTON, J. A. EADES, J. W. STEEDS and G. M. RACKHAM, *Phil. Trans.* **281** (1976) 171.
24. H. J. GOLDSCHMIDT, in "Interstitial Alloys" (Butterworths, London, 1967).
25. M. J. LORETTO, in "Electron Beam Analysis of Materials" (Science Paperbacks, Chapman and Hall, London, 1985) pp. 79–100.
26. O. KUBASCHEWSKI and C. B. ALCOCK, in "Metallurgical Thermochemistry" (Pergamon Press, 1979).

Received 15 October
and accepted 25 November 1985